

Gold Nanoclusters Deposited on SiO₂ via Water as Buffer Layer: CO-IRAS and TPD Characterization

Elad Gross and Micha Asscher*

Department of Physical Chemistry, The Hebrew University of Jerusalem 91904, Israel

Matthew Lundwall and D. Wayne Goodman

Department of Chemistry, Texas A&M University, College Station, Texas 77842

Received: July 11, 2007; In Final Form: August 16, 2007

CO adsorption properties on gold clusters were studied by infrared reflection absorption spectroscopy (IRAS) and temperature-programmed desorption (TPD). Two growth procedures that differ in the final gold clusters morphology were compared. In the first, the clusters were prepared by direct deposition (DD) of gold atoms on SiO₂/Si(100) substrates. The second growth mode is based on initial evaporation of gold atoms on top of amorphous solid water as a buffer layer at 100 K that separates the small gold seed clusters from the substrate. Subsequent annealing to 300 K desorbs the water molecules, resulting in nanocluster growth and their (cold) deposition on the substrate in a buffer layer assisted growth (BLAG) mechanism. It is demonstrated here for the first time that one can independently control cluster size and density by repeating the BLAG procedure as many times as needed. BLAG clusters are more 3D in nature, have larger height to diameter ratio, yet their interaction with CO is very similar to DD clusters. This is reflected by the practically identical CO stretch observed on both clusters at $2106 \pm 2 \text{ cm}^{-1}$. The CO stretch frequency was found BLAG clusters size (2–10 nm) independent. CO molecules that are most strongly bound at the perimeter of the gold clusters do not contribute to the IRAS signal. TPD measurements have shown that CO interaction with BLAG clusters is somewhat weaker than with the DD clusters, indicated by lower and cluster size dependent peak desorption temperature (170–190 K for BLAG vs 230–240 K for DD clusters). Smaller clusters lead to higher CO-desorption temperature. The area under the CO-TPD peak, linearly increases with the number of multiple BLAG cycles. The high-temperature tail of the TPD peaks above 200 K has been correlated with cluster perimeter gold atoms that seem to interact with the underlying SiO₂ substrate.

1. Introduction

Since the discovery of the unique catalytic activity of supported gold nanoclusters, there has been considerable interest in their controlled synthesis.¹ The catalytic activity of these clusters depends on the cluster size and shape; therefore, cluster morphology clearly impacts their catalytic activity.^{1–5} A popular method for deposition of supported metal clusters is based on evaporation of the corresponding metal onto an oxide substrate. The oxide support is often prepared by growing a thin, epitaxial film of the oxide on a metal single crystal closely matched from a crystallography point of view.⁶ The metal atoms diffuse and aggregate on the oxide substrate, initially forming primarily two-dimensional nanoclusters. The cluster density and size distribution obtained via this direct deposition (DD) method depends upon the amount and flux of the evaporated metal, the substrate temperature, and the nature of the support.⁷ Clusters grown by this method are characterized by a relatively narrow size distribution and tend to be flat with an aspect ratio (height to diameter ratio) of ~ 0.2 .^{8–10}

An alternative method for metal cluster growth, introduced by Huang et al.,¹¹ utilizes a xenon buffer layer to separate the evaporated (hot) metal atoms from the cold substrate. Metal atoms are evaporated onto the buffer layer, and, due to the relatively weak interaction with solid xenon, small clusters are

formed by diffusion and aggregation.¹² A subsequent annealing of the sample leads to desorption of the buffer layer, followed by coalesce and growth of the *cold* metal clusters via a buffer layer assisted growth (BLAG) mechanism. The cluster density and size depend on the buffer layer thickness and the amount of evaporated metal via specific power laws.^{11,13} One of the main advantages of this method is that by using a buffer layer, the direct interaction between the hot evaporated metal atoms and the substrate is avoided. For example, Ge particles cannot be prepared by direct deposition on Si(100). Nevertheless, it has been demonstrated that the BLAG procedure yields Ge clusters with a variety of sizes and densities on Si(100).¹⁴

Various atoms and molecular species have been used as efficient buffer materials, including Ar, Kr, CO₂, H₂O,^{15–19} and Xe. BLAG induced clusters are also characterized by a unique morphology. A comparison between DD and BLAG clusters reveal a typical aspect ratio (height to diameter ratio) of ~ 0.2 for the DD clusters, while BLAG aggregates are more 3D in nature, approaching an aspect ratio of ~ 0.5 .¹⁷

To further characterize the BLAG clusters, particularly with respect to the available adsorption sites, CO-IRAS (IRAS = infrared reflection absorption spectroscopy) and CO-TPD (TPD = temperature-programmed desorption) measurements were carried out. These measurements serve as adsorption site titration methods of the exposed surface of the gold clusters. For comparison, identical IR spectroscopic measurements have been

* Corresponding author. E-mail: asscher@fh.huji.ac.il.

carried out for DD prepared clusters. Previous CO-IRAS measurements, where gold was directly deposited onto SiO₂/Mo(110), Al₂O₃/Mo(110), FeO(111)/Pt(111), and HOPG, have always shown a single IR feature at 2100–2130 cm⁻¹, for clusters prepared under somewhat different conditions at room temperature.^{20–23}

CO-TPD measurements were performed for DD gold clusters on a variety of oxides.^{24,25} In these measurements two TPD peaks were identified at ~130 and ~190 K. Density functional theory (DFT) calculations have shown that CO binding energy depends on the specific adsorption site, more sensitively than the stretching vibration of the CO molecule. These theoretical predictions are supported by the apparent contradictory results of TPD (two desorption peaks) and the IR data (single stretch at 2120 cm⁻¹).²³

Decoupling the size and density of metallic clusters on a support is practically impossible to achieve on the basis of a direct deposition growth mode. Here we have introduced a multicycle BLAG procedure for the first time. This procedure leads to variable cluster densities with an essentially constant cluster size distribution, thus decoupling the size and density of supported metallic clusters.

2. Experimental Section

The experiments were carried out in three different ultrahigh-vacuum (UHV) chambers. In one chamber gold clusters were grown on SiO₂/Si(100) (from an n type Si(100) wafer, 0.005 ohm·cm) and characterized ex situ by atomic force microscopy (AFM) and high-resolution scanning electron microscopy (HR-SEM). The SiO₂/Si(100) samples were connected to a liquid nitrogen dewar via two tantalum foils, attached to copper feed-throughs. Ar⁺ ions were used to sputter clean the SiO₂ surface from carbon contaminants; the surface cleanliness was verified by Auger electron spectroscopy (AES). Details on the BLAG method using water-ice as the buffer layer to grow gold clusters and determine their size and density are given elsewhere.¹⁷ In the second chamber, the gold clusters were analyzed in situ by IRAS. A Mo(112) single crystal, spot-welded to Ta wires, could be heated to 1200 K (resistively) or to 2100 K (e-beam bombardment) and cooled to 80 K. The temperature was measured by a W26%Re–W5%Re thermocouple spot welded to the back side of the sample. The Mo sample was cleaned by repeated cycles of oxidation at 1200 K and flashing to 2100 K. Amorphous SiO₂ film was prepared by evaporating 0.5 Å Si onto the sample. The Si layer was subsequently oxidized to SiO₂ by exposure to 5 × 10⁻⁶ Torr of O₂, while the sample temperature was kept at 800 K. By repeating this process, a 6 nm thick amorphous silica film was grown.^{26,27} On top of the SiO₂ film, gold clusters were deposited via the water–BLAG procedure. The cleanliness of the sample and the SiO₂ film was verified by AES measurements. The IRAS instrument had nominal spectral resolution of 4 cm⁻¹ and was equipped with CaF₂ windows. The infrared spectra were collected following exposure to 60 Langmuirs (1 Langmuir = 10⁻⁶ Torr·s) CO at a sample temperature of 80 K.

The third chamber was utilized for CO-TPD from cold (50 K) gold clusters deposited on SiO₂/Si(100). The SiO₂/Si(100) samples were mounted on a closed cycle He cryostat capable of cooling the sample to 50 K and cleaned by Ne⁺ ion sputter. Gold cluster growth and CO-TPD measurements in this chamber were used to compare binding sites and total CO uptake from DD and BLAG deposited gold clusters.

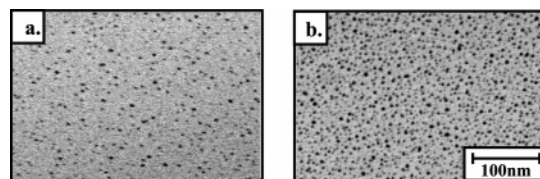


Figure 1. HR-SEM images of Au/SiO₂/Si(100). The gold clusters were grown by one (a) and seven (b) cycles of 0.5 Å Au evaporation on top of 40 monolayers of H₂O at 120 K as a buffer layer, followed by annealing up to 300 K.

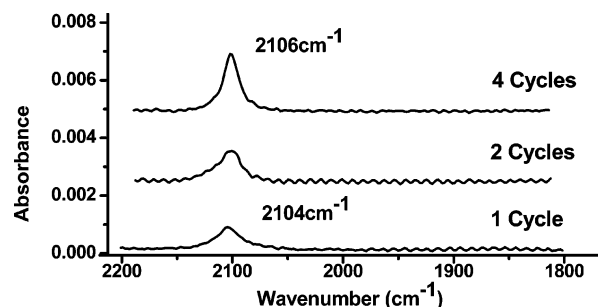


Figure 2. IRAS spectra following 60 Langmuirs exposure of CO (saturation coverage) on gold clusters prepared by one, two, and four cycles of 1.5 Å deposited on 10 monolayers of H₂O as a buffer layer. The IRAS spectra were taken at a substrate temperature of 80 K.

3. Results and Discussion

3.1. CO-IRAS. The size and density of BLAG deposited clusters depend on the buffer layer thickness and the amount of evaporated gold. Figure 1a shows the HR-SEM image of gold clusters on SiO₂/Si(100), deposited by evaporating 0.5 Å Au (determined by quartz microbalance) on top of 40 monolayers of H₂O. The resulting cluster density is $(18 \pm 3) \times 10^{10}$ cm⁻², and their average height is 1.3 ± 0.2 nm. By modifying the buffer layer thickness and the amount of evaporated gold, clusters with specific density and size can be made. With the BLAG method there is an inverse correlation between the size of the clusters and their density,^{11,13,17} similar to DD prepared clusters.^{8–10} One can, however, decouple size and density by utilizing the buffer layer approach. Repeating the BLAG procedure for as many as seven cycles, the gold cluster density has grown linearly with almost no change in clusters size. A seven-cycle procedure where 0.5 Å Au was deposited on top of 40 monolayers of H₂O, then slowly annealed to 300 K, yields a cluster density of $(98 \pm 7) \times 10^{10}$ cm⁻² and 1.6 ± 0.4 nm cluster heights on average (Figure 1b). As can also be seen in the HR-SEM images, a density increase by more than 5-fold has led to a cluster height increase of only 18%. Control over cluster density without affecting the cluster size is unique to the BLAG method.

To characterize the available adsorption sites on BLAG clusters, we have performed IR measurements of adsorbed CO (CO-IRAS). The Au clusters/SiO₂/Mo(112) samples at 80 K were dosed with a saturation exposure of 60 Langmuirs of CO. In Figure 2 IRAS spectra of CO adsorbed on Au/SiO₂/Mo(112) are presented. The gold clusters were prepared by one to four cycles of 1.5 Å Au deposited on top of 10 monolayers of H₂O followed by annealing to 300 K. A cluster density of $(38 \pm 4) \times 10^{10}$ cm⁻² was obtained after the first BLAG cycle with an average height of 1.2 ± 0.2 nm. A single IR absorption peak is evident at 2104 cm⁻¹. A similar stretch frequency was reported in the case of CO on Au(111) atop sites.^{21,22} To study to what extent the IR spectra are sensitive to multiple cycles of the BLAG procedure, IRAS spectra were recorded after one, two,

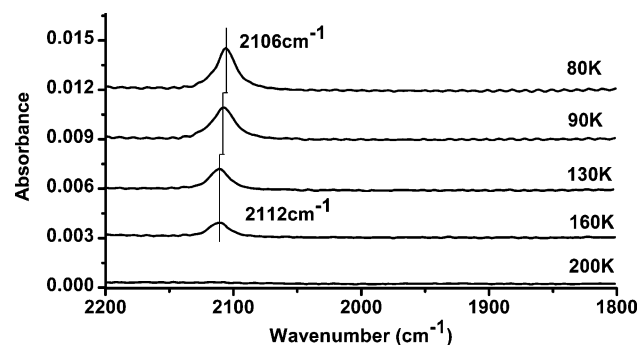


Figure 3. CO-IRAS spectra as a function of temperature. The gold clusters were prepared by six cycles of 1.5 Å Au evaporated on 40 monolayers of H₂O.

and four cycles, as shown in Figure 2. BLAG clusters at densities of $(65 \pm 5) \times 10^{10}$ and $(105 \pm 8) \times 10^{10} \text{ cm}^{-2}$ and heights of 1.1 ± 0.3 and 1.2 ± 0.3 nm were obtained following two and four cycles of evaporation of 1.5 Å Au on 10 monolayers of H₂O and heating to 300 K, respectively.

All three spectra contain only a single IR peak. Increasing the number of cycles from one to four has led to a small shift of the peak from 2104 to 2106 cm⁻¹. In addition, significant changes in the peak profile are observed while increasing the number of BLAG cycles. The measured full width at half-maximum (fwhm) of the peaks is 28, 26, and 17 cm⁻¹ for one, two, and four cycles, respectively. IRAS spectra of clusters prepared by several cycles of 1.5 Å Au evaporation on 40 monolayers of H₂O (instead of 10 monolayers of water, not shown) have led to similar results. In this case the fwhm values were 25, 21, and 18 cm⁻¹ for two, four, and six cycles, respectively. This modification can be attributed to a higher degree of homogeneity of adsorption sites on clusters formed by increasing the number of consecutive cycles. Intercluster repulsive interactions may lead to a reduction in the number of occupied adsorption sites at the cluster perimeter that contribute to IR absorption away from the peak center, in favor of those residing on top.

IRAS spectra as a function of temperature are presented in Figure 3. The gold clusters were prepared by six cycles of 1.5 Å Au on 40 monolayers of H₂O, the clusters density was $(90 \pm 8) \times 10^{10} \text{ cm}^{-2}$, and their average height was 2.2 ± 0.5 nm. At 80 K the IR absorption peak is at 2106 cm⁻¹. The peak intensity decreases while the temperature is increased, and the peak position has gradually shifted to 2112 cm⁻¹ at 160 K. This blue shift at low CO coverage, as a result of partial desorption, is characteristic of CO on Au clusters.^{20–23} It can be attributed to molecules residing on the more strongly bound sites, perhaps at the clusters perimeter, directly interacting with both gold and the SiO₂ substrate.

In Figure 4, IRAS spectra of CO adsorbed on 1.5 Å Au directly deposited on SiO₂/Mo(112) are presented. The cluster density was $(115 \pm 10) \times 10^{10} \text{ cm}^{-2}$, and their average height was 1.0 ± 0.2 nm. In this case the IR absorption peak position at 80 K is 2106 cm⁻¹; however, as the temperature increases to 200 K, the peak shifts to 2120 cm⁻¹. This slightly blue-shifted peak can be assigned to molecules at the clusters perimeter, as explained for the BLAG clusters.

The peak intensities of CO adsorbed on DD clusters are significantly lower than the intensities measured for CO adsorbed on multiple cycled BLAG clusters. However, we note that the spectra in Figure 3 (BLAG) were obtained by evaporation of 9 Å Au (total of six cycles), while the spectra in Figure 4 (DD) are the result of direct deposition of only 1.5 Å Au. To

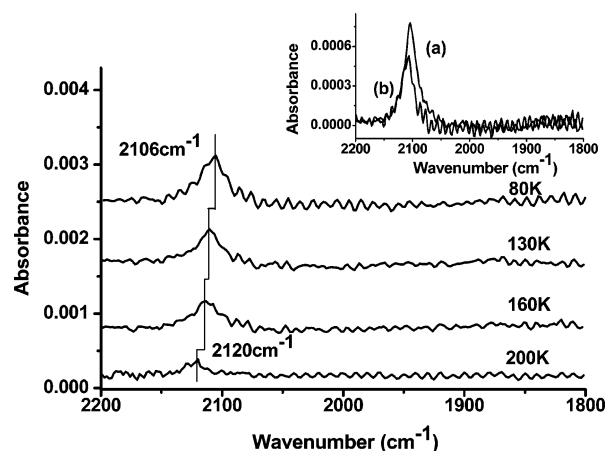


Figure 4. CO-IRAS spectra as a function of temperature. The gold clusters were prepared by direct deposition of 1.5 Å Au on SiO₂/Mo-(112). (Inset) CO-IRAS spectra of gold clusters prepared by 1.5 Å Au directly deposited (a) and via 10 monolayers of H₂O (b). The substrate temperature was 80 K in both cases.

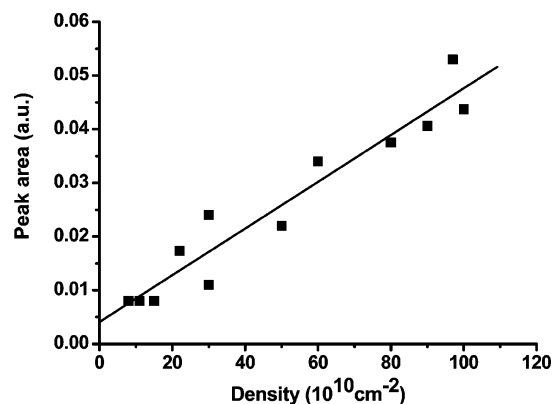


Figure 5. CO-IRAS peak area as a function of cluster density. All the IR spectra were taken at 80 K.

isolate the role of cluster morphology and size on the IR peak position and intensity, the IRAS spectrum of CO adsorbed on BLAG clusters (1.5 Å Au on 10 monolayers of H₂O, Figure 4, inset b) was compared with that from clusters made by direct deposition of 1.5 Å Au on SiO₂ (Figure 4, inset a). The DD clusters are three times denser than a single cycle of BLAG clusters,¹⁷ while the BLAG clusters are larger. Furthermore there is a clear difference in the cluster morphology, since the BLAG clusters have an aspect ratio (height/diameter) of ~ 0.4 , while the DD clusters have an aspect ratio of ~ 0.2 .^{17,18} The DD clusters are denser; however, the IRAS signal intensity of CO adsorbed on these DD clusters is similar to the IRAS signal of CO adsorbed on the less dense BLAG clusters. This may be attributed to a larger number of (yet uncharacterized) cluster-surface imperfections, due to the unique aggregation process and the 3D shape of the BLAG clusters. A somewhat larger sticking probability of CO molecules on such sites may explain the overall more intense IR peak of CO adsorbed on BLAG Au clusters.

A linear correlation was found between the IRAS peak area and the BLAG cluster density (since the IR peak profile/line shape changes with the number of BLAG cycles, one has to measure peak area rather than peak height; Figure 5). Increasing the cluster density leads to a larger overall number of low coordinated atoms, resulting in more CO molecules adsorbed on the BLAG clusters and therefore more intense IRAS signal.

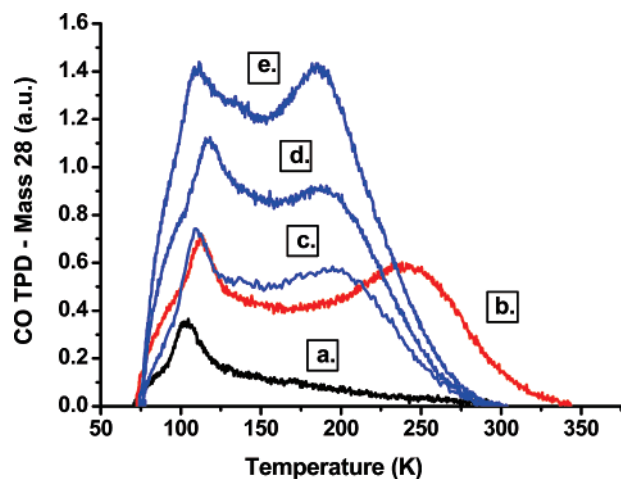


Figure 6. CO-TPD spectra following exposure of 4 Langmuirs of CO, on bare SiO₂ (a, black), 0.5 Å directly deposited on SiO₂ (b, red), BLAG clusters prepared by one (c), two (d) and three (e) cycles of 0.5 Å Au on 40 monolayers of H₂O (blue). The heating rate was 5 K/s throughout.

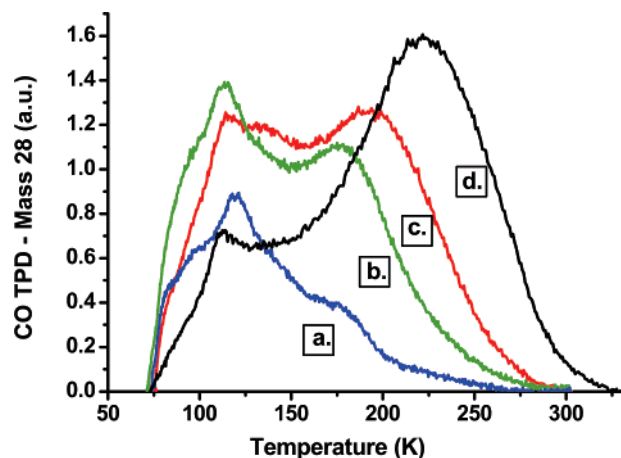


Figure 7. CO-TPD spectra following exposure of 4 Langmuirs of CO on 1.5 Å Au deposited on 100 (a, blue), 40 (b, green), and 10 monolayers of H₂O (c, red) on SiO₂ and 1.5 Å Au directly deposited on SiO₂ (d, black). The heating rate was 5 K/s throughout.

3.2. CO-TPD. To further explore the correlation between the number of BLAG cycles and the actual density of adsorbed CO molecules, we have performed a CO-TPD study from the BLAG grown gold clusters. Adsorption of 4 Langmuirs of CO on bare SiO₂ held at 50 K has led to a single TPD peak at 105 K, with a long tail extending above 250 K (Figure 6a). Evaporation of 0.5 Å gold on bare SiO₂ substrate at 300 K (DD growth mode) followed by exposure of 4 Langmuirs of CO has completely modified the TPD profile (Figure 6b). The TPD peak attributed to CO adsorbed on bare SiO₂ has shifted to 113 K, and a new high-temperature peak emerged at 240 K. This broad peak is assigned to CO molecules adsorbed on gold clusters. CO-TPD spectra from BLAG clusters (0.5 Å gold on top of 40 monolayers of H₂O, 6 nm average cluster diameter¹⁷) resulted in a shift of the high-temperature peak to 190 K, while the low-temperature peak location did not change (Figure 6c). This shift is associated with the size of the gold clusters: Higher desorption temperature pertains to the smaller clusters (Figure 7). Clear evidence for the fact that multiple BLAG results in practically identical TPD, just enhance its intensity, is shown in Figure 6, for a single BLAG cycle (Figure 6c), two cycles (Figure 6d), and three cycles (Figure 6e).

A possible rationalization of the upward shift of the (high-temperature) desorption peak to high temperature as clusters

become smaller is based on the hypothesis that the high-temperature peak position associates with defects at the clusters perimeter that interact with the underlying SiO₂ substrate. As the clusters decrease in their average size, which happens with thinner buffer layers, the total number of these sites increases since the density also increases. One can estimate the total number of gold atoms N_g residing at the clusters' perimeter as follows: $N_g = 2\pi rD/d$, where r is an average cluster radius, D is the corresponding density of clusters prepared by BLAG at that size, and d is the diameter of a single gold atom ($d = 0.288$ nm). $N_g(\text{DD}) = 6.5 \times 10^{13}$ atoms/cm² for DD clusters, and it drops to $N_g(\text{BLAG } 10) = 2.73 \times 10^{13}$ atoms/cm², $N_g(\text{BLAG } 40) = 1.63 \times 10^{13}$ atoms/cm², and $N_g(\text{BLAG } 100) = 0.87 \times 10^{13}$ atoms/cm², for clusters prepared via BLAG on 10, 40, and 100 monolayers thick H₂O buffer layers, respectively. The intensity ratio of the CO-TPD signals at temperatures in the range of 230–280 K (see Figure 7) qualitatively corresponds to the ratio between the numbers of gold atoms at clusters perimeters. This correspondence supports our hypothesis that the high-temperature tail of the CO-TPD spectra originates from defects, steps, or kinks that are at the perimeter of the clusters. The increasing dominance of the sites at the perimeter over those of terraces on top of the clusters as the clusters become smaller in size gradually shifts the desorption peak to higher temperature and makes this peak stronger than the one at 115–120 K, as demonstrated in Figure 7.

The areas under the two TPD spectra (DD (Figure 6b) and single-cycle BLAG, obtained with 10 monolayers of H₂O; not shown) are almost identical, consistent with the CO-IRAS spectra, shown in Figure 4 (inset). However, we note that the DD clusters are three times denser than the corresponding 10 H₂O monolayers-BLAG clusters. This observation leads to a surprising conclusion that the density of CO molecules must be about three times larger on the BLAG clusters than the corresponding density of CO on the DD clusters. It leads to the hypothesis that the sticking probability of CO on BLAG clusters is somewhat larger on BLAG than on DD clusters. One cannot exclude another possibility, that very small clusters formed by the BLAG method and not formed by direct deposition, are invisible by AFM or HR-SEM and these are the source of the surprisingly high CO-TPD intensity.

An interesting observation emerging from Figures 6 and 7 is that the fraction of CO molecules that desorb above 200 K contribute only negligibly to the CO-IRAS signal. This may suggest that the molecules desorbing at temperature above 200 K are associated with surface defects, suggested recently to associate with kink-like sites.²³ Therefore, these molecules may not bind along the surface normal. IR selection rules dictate in such cases that rather small if any contribution to the IR intensity is expected from these adsorbed molecules. This is in spite of the fact that these molecules are more than 25% of the overall CO molecules residing on the Au/SiO₂ surface. This is consistent with a similar explanation used in the literature to justify an apparent discrepancy: There are clearly two CO-TPD peaks while only a single IR absorption is detected.^{22, 25}

CO-TPD peaks at temperatures similar to those reported here were previously shown on a defected planar Au(332) surface and for gold clusters directly deposited on graphite.²³ Similar data were reported for gold clusters on various oxide substrates.^{24,25} These two peaks were attributed to step-like (low-temperature peak) and kink-like (high-temperature peak) sites, supported also by DFT calculations.²³

4. Conclusions

CO adsorption on buffer layer assisted grown (BLAG) and directly deposited (DD) gold clusters on amorphous SiO₂ was studied by CO-IRAS and CO-TPD. Here we examine the importance of various cluster parameters such as size, density, and shape/morphology on their interaction with CO, for better understanding of the mystery of gold catalytic activity and extreme cluster size sensitivity.²

The CO-IRAS stretch frequency was almost identical for cold (160 K) BLAG and DD clusters at 2106 ± 2 cm⁻¹, increasing to 2112 and 2120 cm⁻¹ for BLAG and DD clusters, respectively, upon annealing to 200 K.

Multiple BLAG cycles has been introduced for the first time as a unique procedure to independently control cluster size and density, without intentionally damaging the substrate. This has proven necessary for effective IR and TPD measurements of CO on gold clusters for sizes in the range of 2–10 nm, inspected in this study.

CO-TPD measurements revealed that the CO interaction with DD clusters is stronger than the interaction with BLAG clusters, as indicated by an upward shift of the CO peak desorption temperature. Two TPD peaks observed at 135 and 190 K at higher cluster density are in agreement with previous reports for DD clusters.^{24,25} The more strongly bound CO molecules do not contribute significantly to the IRAS signal. This may arise from molecules at the cluster perimeter that do not bind perpendicular to the surface, consistent with previous IR measurements of CO adsorbed on different oxide substrates.²⁵

BLAG clusters are in general less dense than DD clusters following a single deposition cycle and are characterized by a higher aspect ratio (height to diameter ratio). Both TPD and IRAS measurements have shown that the total number of CO molecules adsorbed on the same amount of gold deposited on SiO₂ is practically identical. The coverage of CO molecules adsorbed per BLAG cluster is, therefore, somewhat higher than that on DD cluster. This might be correlated to the more 3D nature of BLAG clusters which often are assumed to contain more surface steps and kinks. This is in spite of the fact that the interaction between CO molecules and DD clusters is stronger than the interaction between CO molecules and BLAG clusters.

The multiple BLAG procedure, can be utilized to grow several different cluster sizes and more than one type of metallic element on the same substrate. This may prove advantageous for tailored cluster size/multiple-element catalysis. The relevance of different gold clusters morphology for their catalytic activity is currently being studied by employing both UHV and high-pressure approaches.

Acknowledgment. The help of Ori Stein with the TPD measurements is acknowledged. This research was partially supported by a grant from the U.S.–Israel Binational Science Foundation and by the Israel Science Foundation. The Farkas center is supported by the Bundesministerium für Forschung und Technologie and the Minerva Gesellschaft für die Forschung mbh.

References and Notes

- (1) Haruta, M. *Catal. Today* **1997**, 36, 153.
- (2) Valden, M.; Lai, X.; Goodman, D. W. *Science* **1998**, 281, 1647.
- (3) Chen, M. S.; Goodman, D. W. *Catal. Today* **2006**, 111, 22.
- (4) Freund, H. J. *Catal. Today* **2006**, 117, 6.
- (5) Lopez, N.; Janssens, T. V. W.; Clausen, B. S.; Xu, Y.; Mavrikakis, M.; Bligaard, T.; Nørskov, J. K. *J. Catal.* **2004**, 223, 232.
- (6) (a) Freund, H. J. *Angew. Chem., Int. Ed.* **1997**, 36, 452. (b) Street, S. C.; Xu, C.; Goodman, D. W. *Annu. Rev. Phys. Chem.* **1997**, 48, 43.
- (7) (a) Campbell, C. T. *Surf. Sci. Rep.* **1997**, 27, 1. (b) Freund, H. J. *Surf. Sci. Prospect.* **2007**, 601, 1438.
- (8) Kolmakov, A.; Goodman, D. W. *Chem. Rev.* **2002**, 2, 446.
- (9) Lai, X.; St. Clair, T. P.; Valden, M.; Goodman, D. W. *Prog. Surf. Sci.* **1998**, 59, 25.
- (10) Schmidt, A. A.; Eggers, H.; Herwig, K.; Anton, R. *Surf. Sci.* **1996**, 349, 301.
- (11) Huang, L.; Chey, S. J.; Weaver, J. H. *Phys. Rev. Lett.* **1998**, 80, 4095.
- (12) Irawan, T.; Boecker, D.; Ghaleh, F.; Yin, C.; Von Issendorff, B.; Hovel, H. *Appl. Phys. A* **2006**, 82, 81.
- (13) Haley, C.; Weaver, J. H. *Surf. Sci.* **2002**, 518, 243.
- (14) Yoo, K.; Li, A.-P.; Zhang, Z.; Weiering, H. H.; Flack, F.; Lagally, M. G.; Wendelken, J. F. *Surf. Sci.* **2003**, 546, L803.
- (15) Antonov, V. N.; Palmer, J. S.; Bhatti, A. S.; Weaver, J. H. *Phys. Rev. B* **2003**, 68, 205418.
- (16) Waggoner, P. S.; Palmer, J. S.; Antonov, V. N.; Weaver, J. H. *Surf. Sci.* **2005**, 596, 12.
- (17) Gross, E.; Horowitz, Y.; Asscher, M. *Langmuir* **2005**, 21, 8892.
- (18) Liang, G.; Perry, S. P. *Surf. Sci.* **2005**, 594, 132.
- (19) Yan, X.-M.; Ni, J.; Robbins, M.; Park, H. J.; Zhao, W.; White, J. M. *J. Nanopart. Res.* **2002**, 4, 525.
- (20) Luo, K.; Wei, T.; Yi, C. W.; Axnanda, S.; Goodman, D. W. *J. Phys. Chem. B* **2005**, 109, 23517.
- (21) Rainer, D. R.; Xu, C.; Holmblad, P. M.; Goodman, D. W. *J. Vac. Sci. Technol., A* **1997**, 15, 1653.
- (22) Lemire, C.; Meyer, R.; Shaikhutdinov, Sh. K.; Freund, H. J. *Surf. Sci.* **2004**, 552, 27.
- (23) Yim, W. L.; Nowitzki, T.; Necke, M.; Schnars, H.; Nickut, P.; Biener, J.; Biener, M. M.; Zielasek, V.; Al-Shamery, K.; Kluner, T.; Baumer, M. *J. Phys. Chem. C* **2007**, 111, 445.
- (24) Shaikhutdinov, Sh. K.; Meyer, M.; Naschitzki, M.; Baumer, M.; Freund, H. J. *Catal. Lett.* **2003**, 86, 211.
- (25) Lemire, C.; Meyer, R.; Shaikhutdinov, Sh. K.; Freund, H. J. *Angew. Chem., Int. Ed.* **2004**, 43, 118.
- (26) Chen, M. S.; Santra, A. K.; Goodman, D. W. *Phys. Rev. B* **2004**, 69, 155404.
- (27) Luo, K.; Kim, D. Y.; Goodman, D. W. *J. Mol. Catal. A* **2001**, 167, 191.